DYNAMIC SHEAR BEHAVIOR OF A REINFORCED GEOSYNTHETIC CLAY LINER

A Thesis

Presented in Partial Fulfillment of the Requirements for the Degree Bachelor of Science with Distinction in the College of Engineering of The Ohio State University

By

David A. Varathungarajan

*****

The Ohio State University

2006

Honors Examination Committee:

Dr. Patrick Fox, Adviser

Dr. Harold Walker

ABSTRACT

A state-of-the-art, large-scale dynamic direct shear machine has recently been constructed to measure the dynamic shear behavior of geosynthetic clay liners (GCLs). The device is capable of testing specimens measuring 305 × 1067 mm. The device has a maximum shear displacement of 254 mm, a maximum normal stress of 2,400 kPa and is capable of applying a maximum shear stress of 750 kPa. During dynamic operation, the device can sinusoidally shear a specimen to a displacement amplitude of 25 mm at a frequency of 4 Hz.

The dynamic shear behavior of a needle-punched (NP) GCL was studied. To do so, a series of displacement controlled cyclic shear tests were performed on NP GCLs. A testing program was designed to investigate the fundamental dynamic shear behavior of NP GCLs and the post-cyclic static shear behavior of NP GCLs. A baseline test was first conducted at a shear displacement amplitude of 15 mm at 1 Hz for 50 cycles. In subsequent tests, shear amplitude, frequency and number of shear cycles were varied to study the effects these parameters.

Based on the results of the testing program, dynamic shear behavior is governed by the performance of NP reinforcement. As large displacements are approached, additional reinforcement is tensioned and failed, reducing post-cyclic static strength. Additional reinforcement is also failed as the specimen is sheared for an increasing

number of cycles. The effects of cyclic shear frequency are less evident. Additional testing is required to confirm trends in data. Testing has also shown the residual shear strength of NP GCLs is governed by the residual strength of bentonite clay.

This is dedicated to my parents, Rajan and Margaret, and my sister, Rebecca.

ACKNOWLEDGMENTS

I would first like to thank my adviser, Dr. Patrick Fox, for giving me the great opportunity to work on this project. I would also like to thank Chris Nye for his help in preparing data and writing this thesis.

TABLE OF CONTENTS

LIST OF FIGURES

CHAPTER 1

INTRODUCTION

Since the inception of the Resource Conservation and Recovery Act (RCRA), modern solid waste landfills have been required to incorporate lining systems that minimize the movement of water through the waste and into the ground. Without an appropriate liner system, it is possible for contaminated leachate to enter groundwater supplies. Geosynthetic clay liners (GCLs) are often used as a final barrier in composite liner systems. GCLs offer numerous advantages over compacted clay layers for use as a hydraulic barrier, including being more cost effective in many applications.

GCLs consist of a bentonite clay layer bonded to layers of geosynthetic material. In reinforced GCLs, the outer layers of geosynthetics can be connected by stitch-bonded (SB) or needle-punched (NP) fibers that transmit shear stress across the bentonite layer. Such GCLs are used in applications requiring higher shear strengths. While reinforced GCLs offer improved shear strength over unreinforced GCLs, the internal shear strength of the bentonite, the core component of the GCL, remains very weak after hydration. This creates a potential surface for slope failure.

Past research has extensively studied the behavior of GCLs subjected to static loading. However, relatively little research has been conducted which studied the response of GCLs subjected to dynamic loading. For a further discussion of previous

research, see Chapter 2. To appropriately design and assess the long-term performance of landfill liner systems constructed in seismic regions, more information is needed about the shear behavior of liner systems subjected to dynamic loading conditions (USEPA 1995). Since the peak dynamic friction angle is only slightly higher than the peak static friction angle in most instances, static shear strengths are often used for dynamic analyses (Yegian and Lahlaf 1992). Dynamic shear tests are needed to obtain information such as cyclic stress ratio (applied shear stress / static shear strength) versus number of cycles to failure and post-earthquake static shear strengths.

A state-of-the-art, large-scale, dynamic direct shear test machine has recently been constructed to perform such tests. In this thesis, the operation of this device is discussed and results from early dynamic direct shear tests are presented. Displacement controlled cyclic shear tests were performed at various cyclic shear displacement amplitudes, cyclic shear frequencies, and for varying numbers of shear cycles.

CHAPTER 2

REVIEW OF LITERATURE

2.1 INTRODUCTION

Past research has extensively studied the internal and interfacial shear strength of GCLs and various liners systems under static conditions. Less information is available on the dynamic behavior of liner systems, especially the internal shear behavior of GCLs. This chapter provides a brief review of: 1) current laboratory devices for shear testing of geosynthetics, 2) internal static shear behavior of GCLs, 3) considerations for the laboratory measurement of GCL shear strength, and 4) dynamic shear behavior of GCLs.

2.2 TESTING DEVICES AND PROCEDURES

Laboratory testing of geosynthetic shear strength is complicated by issues such as material variability, anisotropy, machine friction, and many other factors. In this section, some of the devices used to measure internal strengths of GCLs are discussed.

2.2.1 DIRECT SHEAR

Direct shear is the primary method used for measuring internal and interfacial shear strengths of GCLs. The standard direct shear test for geosynthetics and GCLs is described in ASTM D 5321 and ASTM D 6234, respectively. Specimens are placed in a

shear box where either the upper or lower half of the box translates laterally relative to the other, shearing the specimen. A schematic of this setup is shown in Figure 2.1. ASTM standards require a minimum specimen size of 300 mm x 300 mm in order to minimize edge effects. The device must also be capable of operating at a constant displacement rate (strain controlled) or at a constant shear stress (stress controlled) and maintaining constant normal stress. When testing GCLs, the specimen must have access to water in order to maintain complete hydration during testing.

Direct shear devices have the advantage of shearing the specimen in one direction, which closely imitates conditions in the field. This helps reduce any effects associated with specimen anisotropy. Specimens can also be relatively large, providing more accurate results. However, direct shear tests utilizing a 300 mm x 300 mm sample are too small to measure residual conditions of most GCLs and GCL interfaces (Fox and Stark 2004). To measure residual strengths, a capacity for large shear displacements is required. In addition, typical direct shear devices do not maintain a constant shearing area during testing. This can be remedied by using a longer shearing block which travels into the test chamber during shearing. However, doing so allows previously unconsolidated and unsheared material to enter the failure surface. The direct shear test also has the disadvantage of requiring an adequate gripping system to transfer shear stress to the specimen. The effectiveness of the gripping system substantially affects the quality of test results (Fox et al. 1997). End clamping may also be employed to ensure failure at the desired interface; however, this may cause an uneven shear stress distribution in the specimen, leading to progressive failure effects.

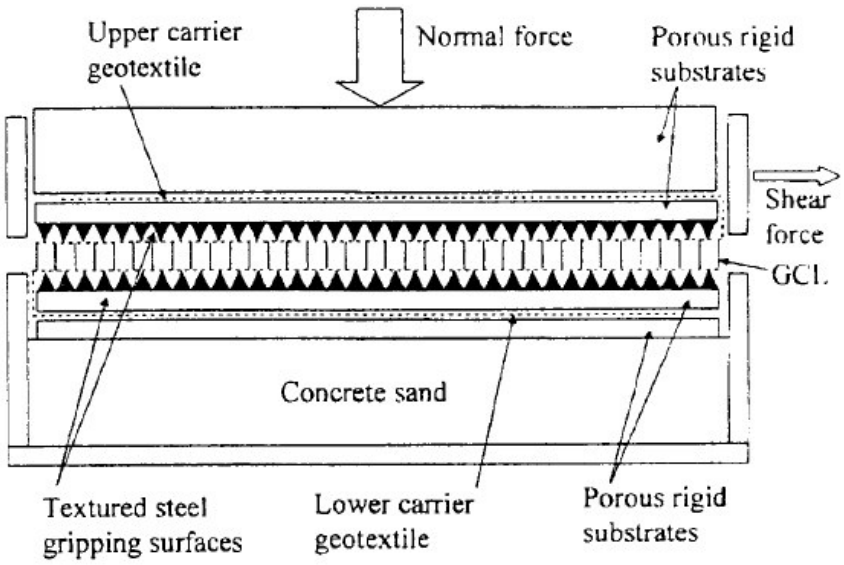

Figure 2.1: Typical direct shear device (Zornberg et al. 2005).

2.2.2 TORSIONAL RING SHEAR

When compared to a direct shear machine, a torsional ring shear device offers the advantage of having the capacity to measure residual strengths (Eid and Stark 1997). This is achieved by the device's ability to shear a specimen over an unlimited shear displacement. In some cases, the measurement of residual strengths may require more than 1 m of displacement (Stark and Poeppel 1994). A schematic of a torsional ring shear device is shown in Figure 2.2. Annular specimens are placed in the device with a shaft passing through the center. Normal stress is applied as the specimens are rotated about the shaft. Applied torque and cumulative displacement are measured. Since the specimen is annular in shape, displacements are not equal in all parts of the specimen. This can result in an uneven stress distribution and thus progressive failure effects, especially in specimens exhibiting strong anisotropy (Gilbert et al. 1995).

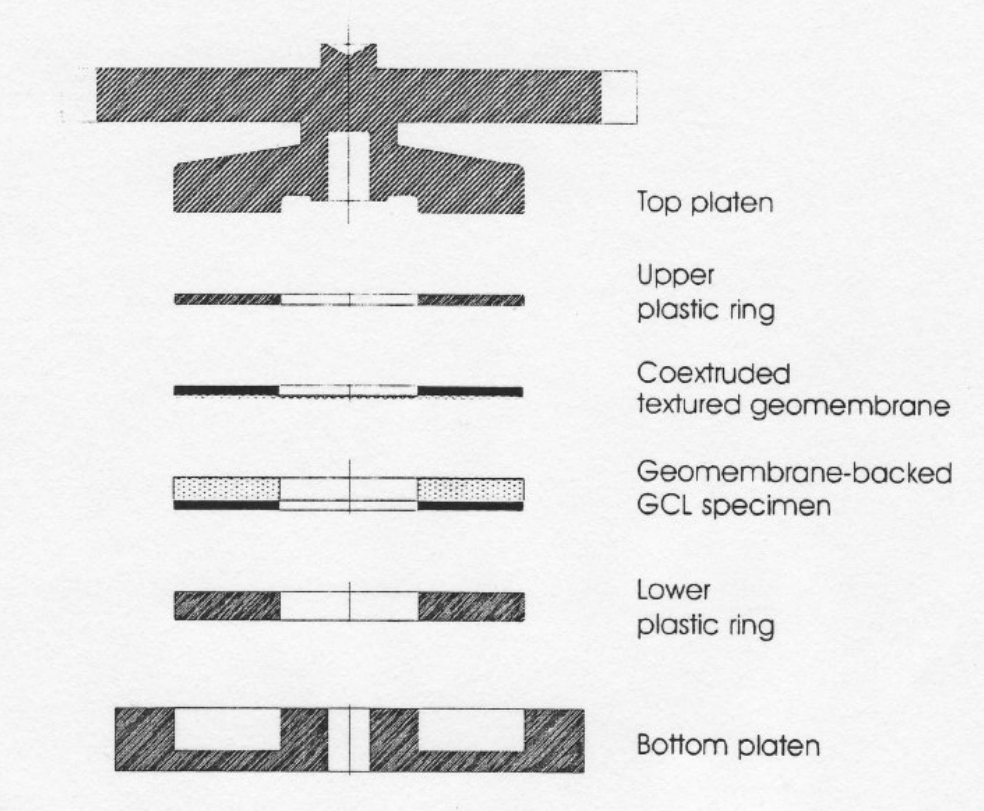

Figure 2.2: Schematic of torsional ring shear device (Eid and Stark 1997).

2.3 INTERNAL STATIC SHEAR BEHAVIOR OF GCLs

Fox et al. (1998) performed direct shear tests on three hydrated GCLs: a geomembrane (GM) supported unreinforced GCL (GCL-1), a stitch-bonded (SB) GCL (GCL-2) and a needle-punched (NP) GCL (GCL-3). The tests were conducted at normal stress levels ranging from 6.9 to 279 kPa. The stress-displacement curves from tests at 141 kPa are presented in Figure 2.3. The reinforced specimens reached peak strengths then demonstrated clear strain-softening as residual conditions were approached. This behavior was less dramatic in the unreinforced GCL. The unreinforced GCL (GCL-1) quickly reached peak strength at a displacement of 1.4 mm. The reinforced GCLs required significantly larger displacements to reach peak strengths as needle-punched and

stitch-bonded reinforcements were engaged (39.7 mm for GCL-2, 22.9 mm for GCL-3). All three specimens had similar residual strengths, suggesting reinforcement does not contribute to residual strength. This behavior was also observed by Chiu and Fox (2004) and Zornberg et al. (2005).

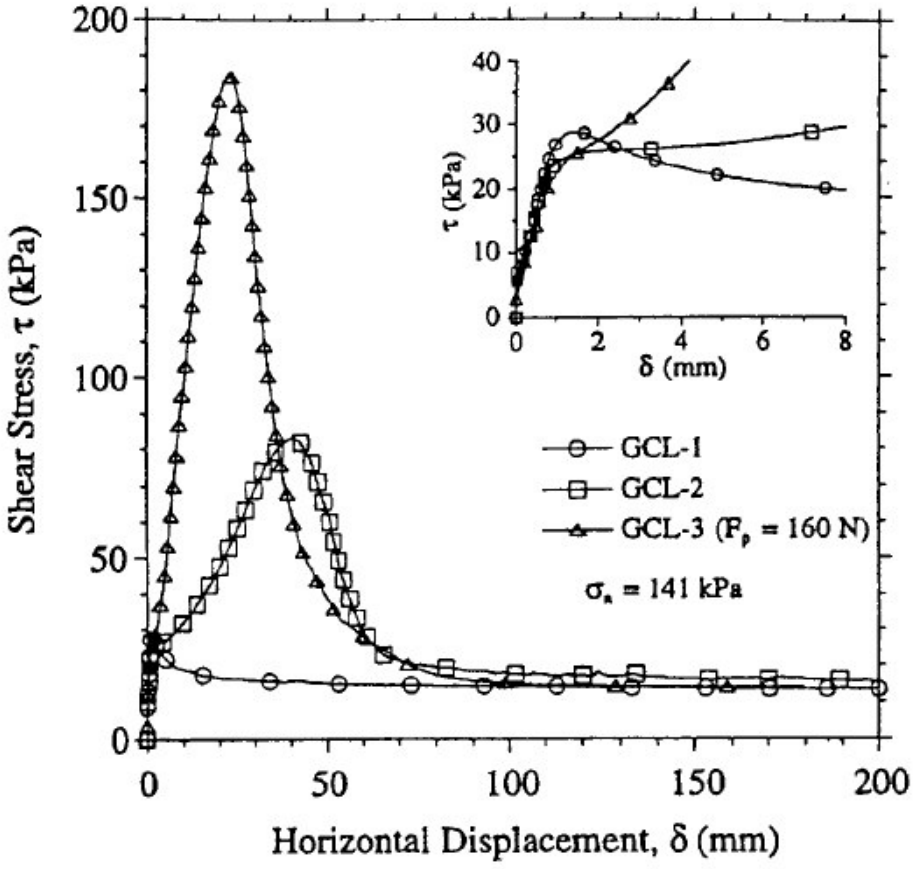

Figure 2.3: Stress-displacement curves for unreinforced (GCL-1), stitch-bonded (GCL-2) and needle-punched (GCL-3) geosynthetic clay liners (Fox et al. 1998).

2.4 LABORATORY MEASUREMENT OF GCL SHEAR STRENGTH

The standard procedure for testing internal and interfacial shear strengths of GCLs with a direct shear machine is described in ASTM D 6243. The method calls for a minimum specimen size of 300 mm × 300 mm (square or rectangular specimens are

recommended). The specimen should be sheared between two blocks covered with an aggressive gripping surface capable of transferring shear stress to the specimen. End clamping is also permitted so long as it does not interfere with measured strengths. ASTM D 6243 also specifies a maximum displacement rate of 1 mm/min. if excess pore pressures are not expected to develop. If excess pore pressures are expected, a procedure is outlined to calculate a maximum displacement rate. After shearing, the specimen should be inspected for failure location, failure mechanism and any local distress caused by the gripping/clamping system. Issues such as specimen conditioning, hydration procedure, testing normal stress and testing configuration are not specified by ASTM D 6243, leaving such parameters for the user to define.

2.4.1 SPECIMEN SIZE

Compared to direct shear tests performed on natural soils, GCLs require larger test specimens. Fox and Stark (2004) attribute this to the fact that:

- larger shear displacements are often required to reach peak strength and residual strength conditions;
- textured elements of many geosynthetics (e.g. geonet, textured geomembrane) are larger than for most soils; and
- the spacing of some types of GCL reinforcement (e.g. SB) may be as large as 100 mm.

Large specimens also reduce edge effects and local variability in material strength. However, large specimens have the disadvantage of requiring larger, more expensive

testing equipment. Tests can also become difficult to perform and maximum normal stress can be limited (Fox and Stark 2004). This has led some researchers to compliment large scale tests with tests on smaller specimens (Stark and Eid 1996, Gilbert et al. 1997).

2.4.2 GRIPPING AND CLAMPING SYSTEM

Fox and Stark (2004) also discussed specimen clamping/gripping systems. To ensure the most accurate shear strength data is obtained, shear displacement must be uniform at all points on the failure surface. Depending on the gripping system, the intended failure surface may not have the lowest shear resistance and failure may occur elsewhere (e.g. between the specimen and the gripping surface). Fox et al. (1997) addressed the effectiveness of various gripping systems. In their research, three different static shear tests were conducted with different gripping systems on an NP GCL. The resulting stress-displacement curves are shown in Figure 2.4.

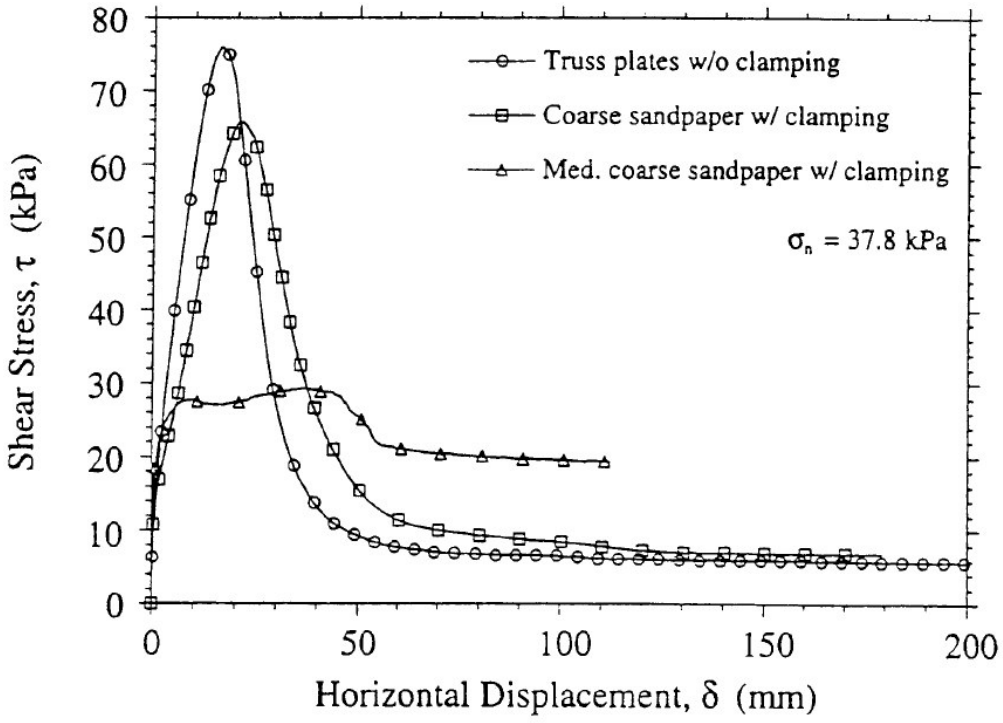

Figure 2.4: Stress-displacement curves of NP GCL with various gripping surfaces (Fox et al. 1997).

For the lowermost curve, the specimen was clamped at the ends and the gripping surface consisted of medium coarse sandpaper. Significant stretching of the GCL at the clamp was observed. A similar test was performed using coarser sandpaper and the same clamping procedure. Some slipping did occur along the GCL-sandpaper interface, but the GCL did fail internally. A final test was performed using no end clamping and a modified steel truss plate used in wood construction for the gripping surface. The truss plate had aggressive metal teeth machined to a maximum height of 2 mm. This system yielded an internal GCL failure with no slipping. Compared to the other systems, the metal truss plate produced the largest peak strength and slightly lower residual strength.

2.4.3 FAILURE ENVELOPE SELECTION

Normal stress is another parameter determined by the user. Since shear behavior is extremely dependent on applied normal stress and failure envelopes are often non-linear, it is important to select an appropriate range based on anticipated field conditions (Chiu and Fox 2004). GCLs used in the bottom layers of liner systems are initially subjected to low normal stresses which increase with time. For such applications, tests should be performed over a wide range of normal stresses. However, GCLs used in cover liner systems are subjected to low normal stresses throughout design life, making a narrow normal stress range more appropriate for testing. Typically, failure envelopes are simplified to a linear envelope composed of a cohesion intercept and a friction angle. This envelope is only valid within the range of normal stresses at which the tests were conducted.

2.4.4 SPECIMEN HYDRATION

Unless a GCL is expected to be encapsulated between two geomembranes, full hydration is always expected in the field (Gilbert et al. 1997). Therefore, testing should be conducted under hydrated condition when hydration is expected. This is an important aspect of the test as previous research has shown GCL strength is highly dependent on the hydration conditions (Stark and Eid 1996, Eid and Stark 1997, Zornberg et al. 2005). The hydration liquid itself can also significantly affect GCL shear strengths. Tap water is typically used due to convenience and its chemistry being comparable to typical pore water in most soils. A site specific liquid may also be used (Fox and Stark 2004).

Specimens are commonly hydrated and consolidated inside the shearing device until volume change ceases. This procedure may require up to three weeks in some cases (Gilbert et al. 1996, Stark and Eid 1996). Fox et al. (1998) developed a time-saving accelerated hydration procedure. Under this method, the specimen is hydrated outside of the shearing machine for two days under a low normal stress (1 kPa) with just enough water to reach the expected final hydrated water content (estimated from previous tests). The specimen is then placed in the testing device and provided free access to water under the desired normal stress for two additional days. Using this method, most GCLs attain equilibrium in less than twenty-four hours (Fox et al. 1998, Triplett and Fox 2001, Nye 2006).

2.5 DYNAMIC SHEAR BEHAVIOR OF GCLS

Previous research has focused on the dynamic interfacial shear behavior of geosynthetics (e.g. Yegian and Lahlaf 1992, Yegian et al. 1995, De and Zimmie 1998, Yegian and Kadakal 1998). Much less research has been conducted on the dynamic shear behavior of GCLs. Kim et al. (2005) and Lo Grasso et al. (2002) investigated the dynamic shear behavior of GCL/geomembrane interfaces using shake tables and Lai et al. (1998) published the only study available on the effects of cyclic loading on the internal shear strength of a GCL.

Lai et al. (1998) conducted direct simple shear tests on an unreinforced, geomembrane-supported GCL for both static and cyclic loading. Circular specimens measuring 80 mm in diameter were tested under dry and hydrated conditions. Under dry conditions, normal stress ranged from 23 to 320 kPa. Under hydrated conditions, normal

stress ranged from 23 to 113 kPa. The gripping system used several 16-gauge brass nails embedded in the geomembrane to force shear failure to occur within the bentonite. Stress controlled tests were conducted at select cyclic stress ratios (ratio of cyclic shear stress to undrained static shear strength). Since the tests were performed in a stress-controlled mode, post-peak behavior could not be obtained. As a result, all reported data refers to peak shear strengths.

When considering the specimens tested under dry conditions, Lai et al. observed that for cyclic stress ratios less than 1.0, failure did not occur after 200 cycles. In fact, post-dynamic shear strength increased proportionally to the applied cyclic stress ratio. This behavior was attributed to densification of bentonite during cyclic loading. Subsequent tests also showed that shearing frequency had no effect on post-cyclic static strengths for the dry condition.

Static and cyclic shear tests were then performed on hydrated GCLs. Five cyclic tests were performed at a normal stress of 45 kPa with frequency of 0.09 Hz while the cyclic stress ratio ranged from 0.53 to 0.92. At a cyclic stress ratio of 0.53, the specimen did not fail after 200 cycles. When the cyclic stress ratio was increased to 0.67, the specimen failed after 32 cycles. Stress-displacement curves from these tests are presented in Figure 2.5. Contrary to the dry specimen, as the number of cycles increased, shear displacement also increased.

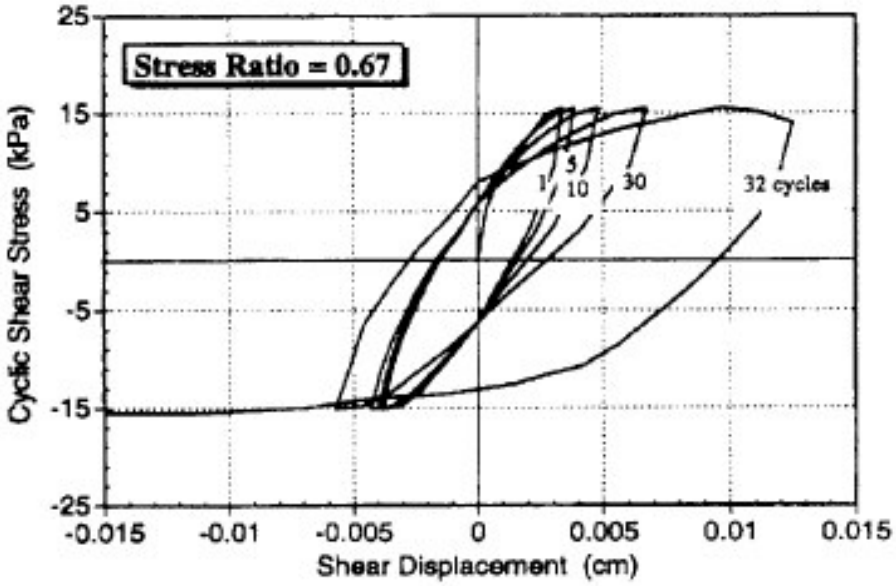

Figure 2.5: Cyclic shear stress-displacement curves for hydrated GCL (Lai et al. 1998).

Lai et al. also presented a comparison of the results from the hydrated GCL tests to cyclic shear tests conducted on natural clay soils. The results showed shear strength decreased with an increasing number of cycles. This reduction was not as severe in the GCL as it was in the natural soils. These results are shown in Figure 2.6.

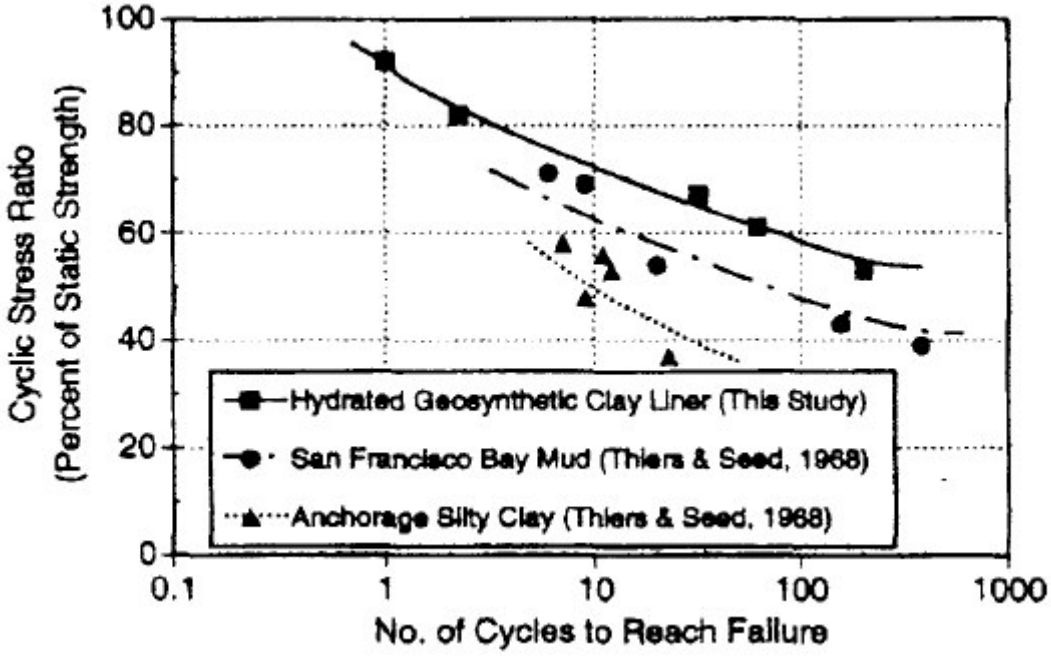

Figure 2.6: Effects of cyclic loading on shear strengths of natural soils and hydrated GCL (Lai et al. 1998).

CHAPTER 3

DESCRIPTION OF TESTING EQUIPMENT

3.1 DYNAMIC DIRECT SHEAR MACHINE

In response to the need for more information about the dynamic shear behavior of GCLs, a state-of-the-art, large scale direct shear machine has been constructed to investigate the shear behavior of GCLs and liner systems. The device measures 3.8 m long, 1.0 m wide and 1.2 m tall. The design of the machine is similar to that of the static direct shear machine described by Fox et al. (1997) with the exception that the machine is capable of applying bi-directional dynamic loads to a test specimen. A picture of the machine is shown in Figure 3.1. Scale drawings are also shown in Figure 3.2 (a) and (b), providing plan and profile views along with a detailed view of the test chamber. The test chamber measures 305 × 1067 mm and can accommodate specimens up to 254 mm in thickness. A specimen is placed in the test chamber and sheared by a hydraulic actuator placed in front of the test chamber. A maximum shear displacement of 254 mm is possible, allowing measurement of residual shear strengths in most cases (Fox et al. 1998, Triplett and Fox 2001).

Figure 3.1: Dynamic direct shear machine.

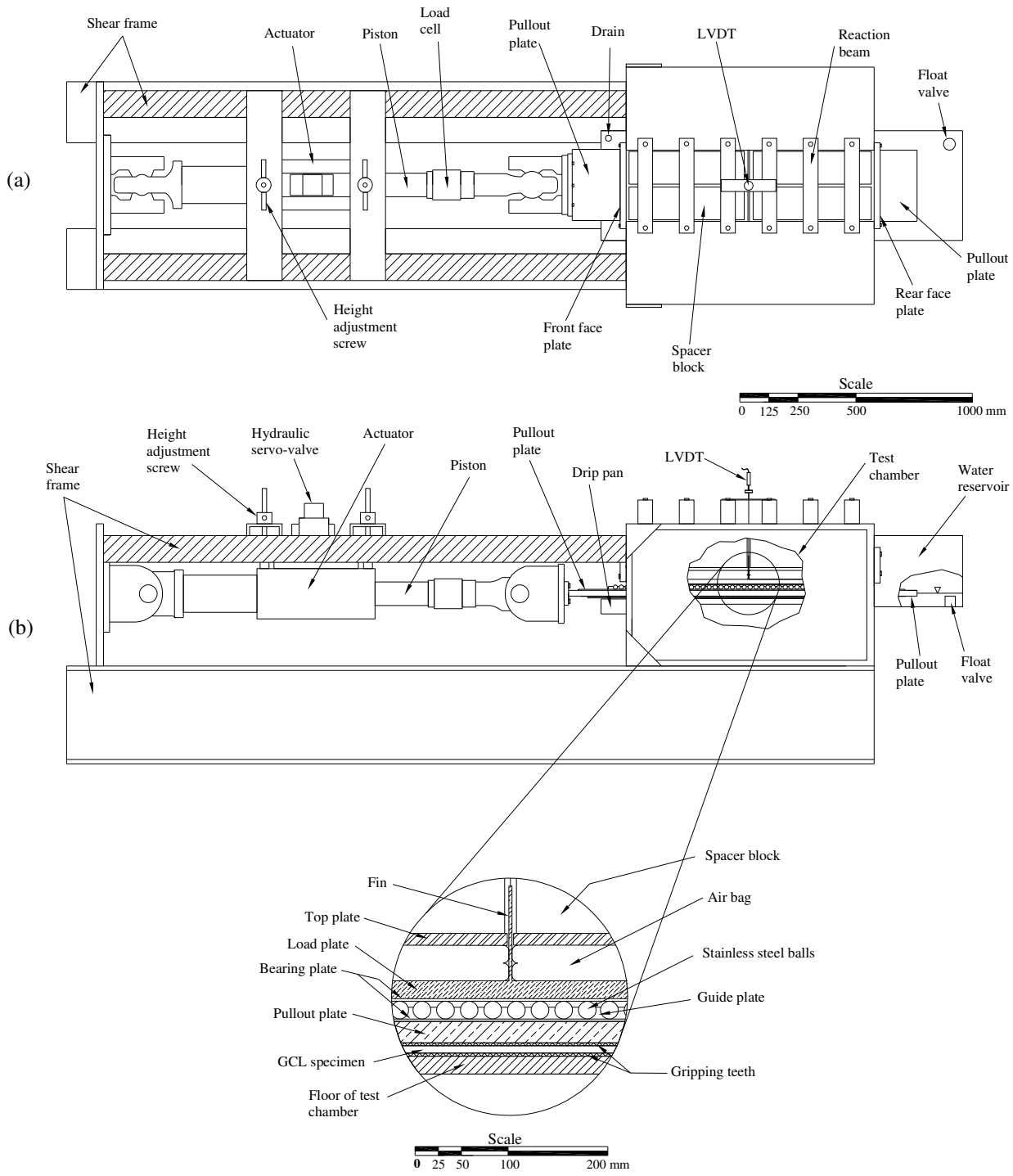

Figure 3.2: Dynamic direct shear machine, (a) plan view and (b) profile view (Fox et al. 2005).

3.1.1 SHEARING SYSTEM

Shear stress is applied to the specimen using a hydraulic actuator with a capacity of 245 kN, which corresponds to an applied shear stress of 750 kPa. An axial load cell designed for cyclic loading is incorporated into the piston of the actuator to measure applied shear forces on the test specimen. The actuator is driven by a 340 liter/min. hydraulic power unit and a hydraulic manifold that allows 19 liters of accumulation to improve actuator response during cyclic operation. The actuator is controlled by a three-stage servo-hydraulic valve and an MTS FlexTest SE digital controller connected to a PC running MTS 793 software. This control setup allows essentially any displacement-controlled or stress-controlled time history to be run. For static shear tests, the system is capable of shear displacement rates as slow as 0.01 mm/min. This displacement rate is ten times slower than the maximum displacement rate recommended by Fox et al. (2004) for internal shear of hydrated GCLs. During sinusoidal cyclic operation, the actuator is capable of a displacement amplitude of 25 mm at a frequency of 4 Hz.

Shear forces are applied to the test specimen by a coated aluminum pullout plate measuring 1500 x 305 x 22 mm. The pullout plate is bolted to the actuator at the front of the test chamber. Due to the mass of the pullout plate, inertial effects can be seen in specimens sheared sinusoidally at frequencies greater than 4 Hz. The pullout plate is 433 mm longer than the test chamber, 152 mm of which is required for attachment to the actuator. The remaining 281 mm allows the pullout plate to enter the rear of the chamber and maintain a constant shearing surface area throughout testing. An aggressive gripping surface is attached to the bottom of the pullout plate. This gripping surface is constructed of modified metal connector plates (i.e., truss plates) used in wood truss construction,

similar to those described by Fox et al. (1997). The plates have been modified by cutting the teeth to a height of 1-2 mm with a flat profile, allowing them to grip the specimen in both directions during cyclic loading. Channels have been machined in the underside of the pullout plate to allow the specimen adequate access to water and to allow for drainage. In most cases, the gripping system eliminates the need to end-clamp specimens, allowing the specimen to fail along the weakest surface and avoiding progressive failure effects (Fox and Stark 2004).

3.1.2 NORMAL STRESS AND VERTICAL DISPLACEMENT SYSTEMS

The normal stress system is capable of applying a maximum normal stress of 2,000 kPa, corresponding to a landfill approaching 150 m in depth. Normal stress is developed in two air bags resting on a rigid load plate. Below the load plate, a layer of 517 free-rolling ball bearings reduces friction on the pullout plate to 2% of the applied normal force (Schiethe 1996). The airbags used in the machine are bellowed to prevent tensioning of the rubber as the bags inflate, which would cause a decrease in the applied normal stress. Each airbag reacts against an aluminum top-plate, which reacts against three aluminum reaction beams bolted transversely across the test chamber. Wooden spacer blocks of different sizes, depending on the thickness of the specimen, are used to fill the void space between the reaction beams and top plate. The airbags are separated by a metal fin attached to the load plate. On the ends of the test chamber, the airbags are restrained laterally by face plates. Vertical displacement of the load plate associated with volume change in the specimen is continuously monitored during all stages of testing using a linear variable displacement transducer (LVDT). The LVDT is held by a frame

which is attached to the top of two reaction beams. Motion from the load plate is transferred to the LVDT by a brass rod which rests on the fin.

Due to the potential for rapid volume change during cyclic shearing of specimens, the air pressure system must have the ability to maintain constant pressure under such conditions. An air amplifier is used to increase the building-supplied air by a factor of four to a maximum of 2500 kPa. The amplifier feeds a pair of 18 liter air tanks located beneath the test chamber. Air fills the primary tank and passes through a regulator which fills a secondary tank at the desired lower pressure for testing. The secondary tank is connected to the air bags with flexible rubber hosing. This allows the air bags to have access to a reserve supply of air at the appropriate pressure. Air pressure in the secondary tank and air bags is measured using a 2100 kPa digital test gage. The components below the airbags add an additional 2.9 kPa to the applied normal stress.

3.1.3 HYDRATION SYSTEM

A water reservoir at the rear of the test chamber provides the specimen with constant access to water during all stages of testing. The pullout plate has longitudinal channels milled into the underside and the truss plates have holes across their surfaces to allow for water drainage. A layer of coarse wire mesh separates the pullout plate and the truss plates to prevent clogging of the water channels. The bottom of the test chamber uses a similar system to provide drainage to the underside of the specimen. A drip pan at the front of the machine collects and drains excess water from the test chamber.

3.1.4 DATA AQUISITION

The dynamic direct shear machine uses a process control and data acquisition system developed by MTS for operation of the actuator. The FlexTest SE digital controller monitors the hydraulic power unit, manifold, servo-hydraulic valve, load cell, and LVDT. The controller is connected to a personal computer, giving the user complete control of the testing system, including pump function, piston motion and data sampling.

CHAPTER 4

TESTING PROGRAM AND RESULTS

The testing program was designed to investigate 1) the fundamental dynamic shear behavior of NP GCLs and 2) the post-cyclic static shear behavior of NP GCLs. Specifically, the program focused on:

- analyzing the mechanisms of failure for GCLs under dynamic shear conditions, and
- determining the effects of varying cyclic shear displacement amplitude, frequency and number of cycles on dynamic and post-dynamic shear behavior.

The GCL product used for this research is Bentomat ST, manufactured by CETCO of Arlington Heights, Illinois. This GCL consists of a bentonite layer surrounded by an upper woven geotextile and by a lower nonwoven geotextile Needle-punched fibers are used to reinforce the GCL. A cross section of Bentomat ST is shown in Figure 4.1.

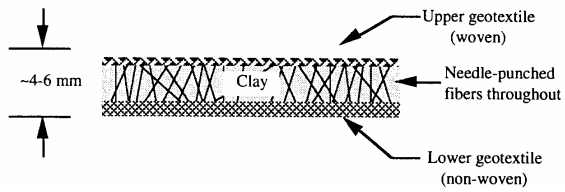

Figure 4.1: Bentomat ST cross section (Rowland 1997).

4.1 TESTING PROCEDURE

When testing the shear strength of GCLs, hydration of the specimen has significant effects on the specimen's strength. Full hydration should be expected in the field unless the bentonite is encapsulated between two geomembranes (Gilbert et al. 1997). The GCL should always be sheared under hydrated conditions when hydration is expected in the field (Fox et al. 1998). All specimens tested were hydrated using the accelerated, two-stage procedure described by Fox et al. (1998). The specimen was first hydrated with just enough water to reach the expected final water content (160%) under very low normal stress for two days. The specimen was then placed in the test chamber under the desired normal stress of 141 kPa, given free access to water for two days and allowed to consolidate. During this stage, vertical displacement was measured.

After completing the hydration procedure, displacement controlled cyclic shear tests were performed. Upon completion of the cyclic shear test, the pullout plate was disconnected from the actuator, removing any shear stress in the specimen, and the specimen was left in the machine under the desired normal stress for 24 hours while vertical displacement was measured. This allowed any excess pore pressures developed during cyclic shearing to dissipate. A static shear test was then conducted at a shear displacement rate of 0.1 mm/min for 200 mm. The specimen was then removed from the machine, examined, and water content measured.

An initial, baseline cyclic shear test was performed at an amplitude of 15 mm and a frequency of 1 Hz for 50 cycles, with the actuator following a sinusoidal wave. To study the effects of varying cyclic-shear amplitude, displacement controlled cyclic shear tests were performed at amplitudes of 5, 10, 15, 20, and 25 mm at a frequency of 1 Hz for

50 seconds. To study the effects of varying the cyclic-shear frequency, tests were performed at an amplitude of 15 mm for 50 cycles with frequencies of 0.1, 0.5, 1.0, 2.0, and 3.0 Hz. A static test was also performed without prior cyclic loading for comparison. To study the effects of varying the number of cycles, tests were performed at 15 mm amplitude with a frequency of 1 Hz for 10, 50 and 100 cycles.

4.2 TESTING RESULTS

4.2.1 BASELINE TESTING RESULTS

Results from the baseline test are presented in this section. Figure 4.2 is a plot of vertical displacement versus time during the second stage of hydration. The first point on the curve represents the relative position of the load plate prior to application of the normal stress and is equal to zero. As the normal stress is applied, the load plate rapidly moves downward. This movement is a combination of seating of the machine parts due to the gripping teeth seating into the specimen and removal of air from the unsaturated specimen. However, these quantities cannot be separated, thus only relative vertical movements should be examined (Rowland 1997).

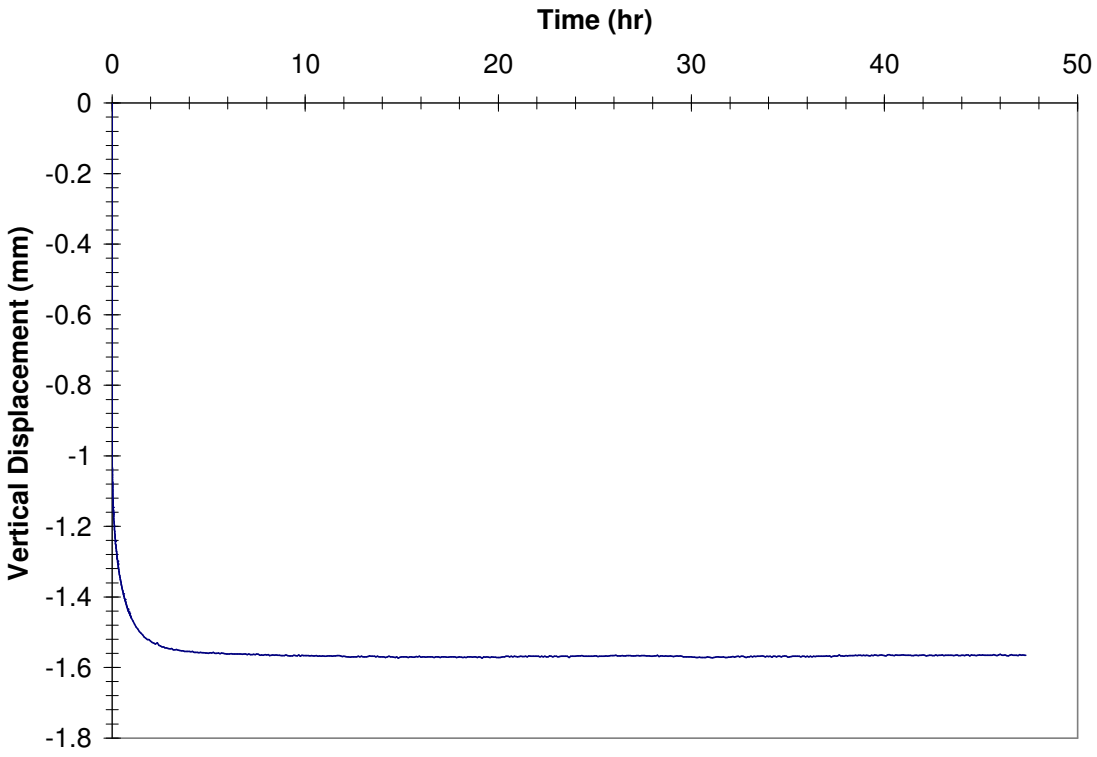

Figure 4.2: Second stage hydration data for baseline cyclic shear test.

Figure 4.2 shows that the specimen quickly came to equilibrium (within 5 hours), which is consistent with the specimen being placed in the test chamber at the expected final water content of 160%. Based on vertical displacement, a second stage hydration time of 48 hours proved to be excessive after looking at other hydrations performed at 141 kPa.

After the specimen was fully hydrated, it was sheared at a displacement amplitude of 15 mm at a frequency of 1 Hz for 50 seconds. A plot of shear stress versus time for this test is shown in Figure 4.3. Shear stress is also plotted as a function of displacement in Figure 4.4. A plot of vertical displacement during the cyclic shearing is shown in Figure 4.5.

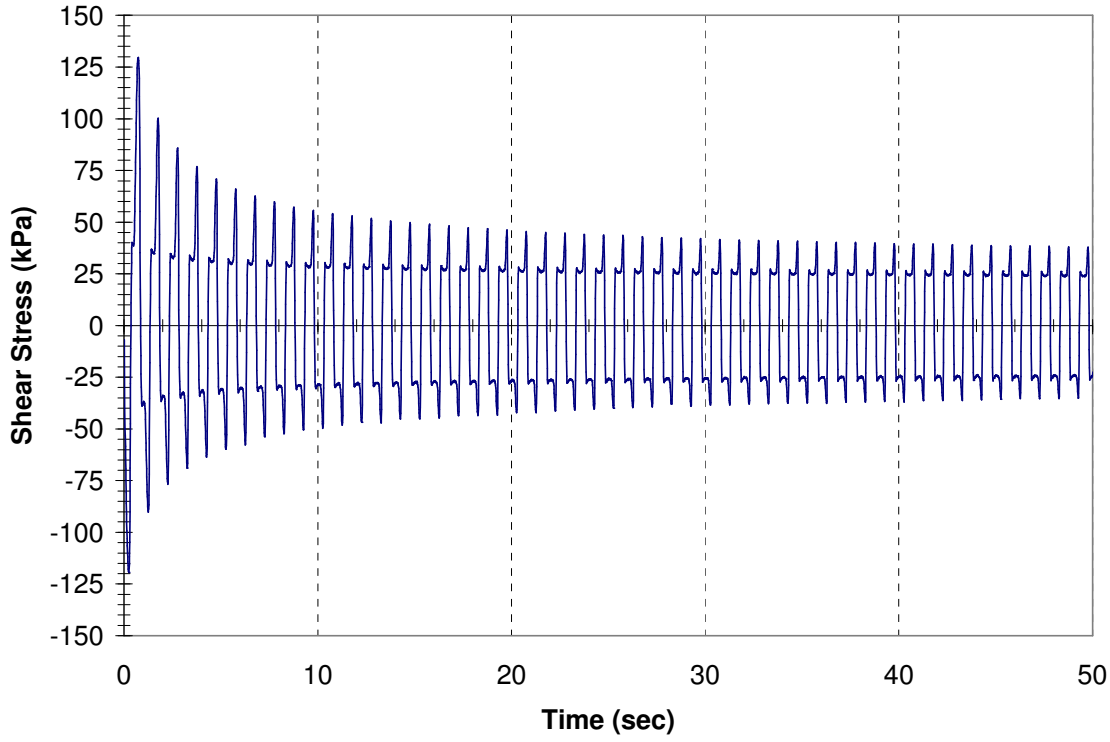

Figure 4.3: Shear stress versus time for baseline cyclic shear test.

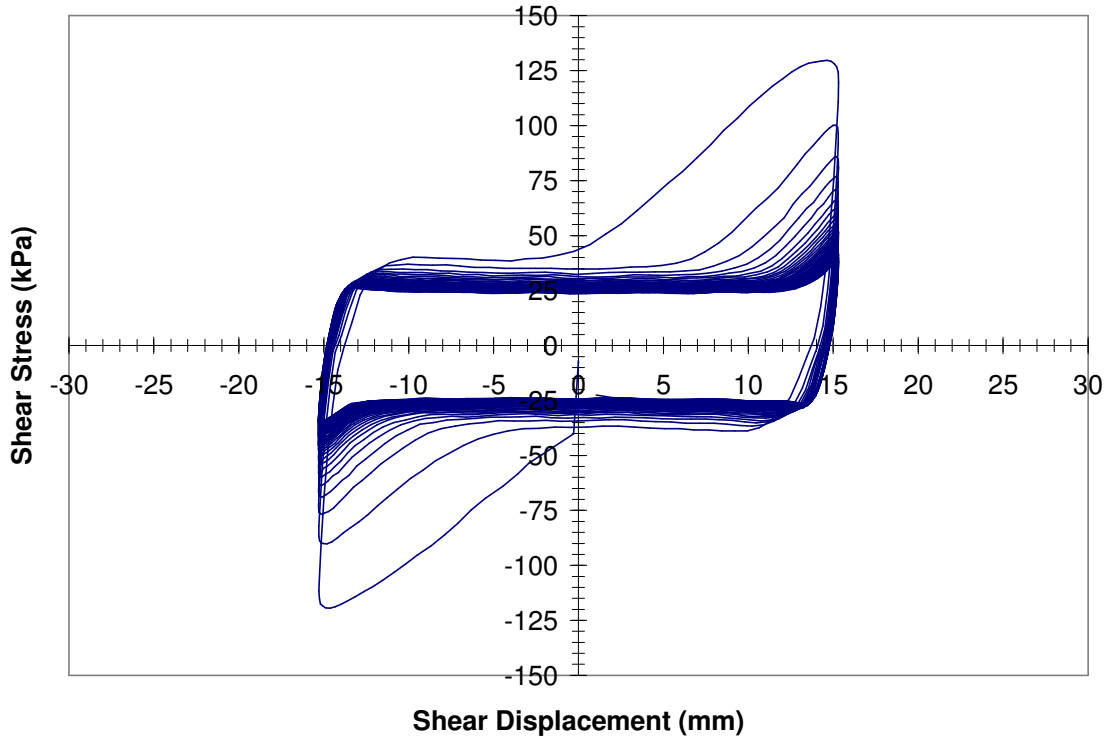

Figure 4.4: Shear stress versus displacement for baseline cyclic shear test.

During the first cycle, shear stress reached a maximum value of 129 kPa. The peak shear stress for this cycle was achieved at a displacement just prior to the maximum amplitude. Shear stress decreased non-linearly during subsequent cycles until reaching a near-steady value of 37 kPa at the 50th cycle. Interestingly, shear stress increased sharply as maximum displacement was approached and reinforcement was engaged. This behavior differs from that typical of natural soils (Kramer 1996).

GCL volume change data is presented in Figure 4.5. After undergoing some initial expansion, the specimen contracted in a non-linear fashion with respect to time and loading cycle.

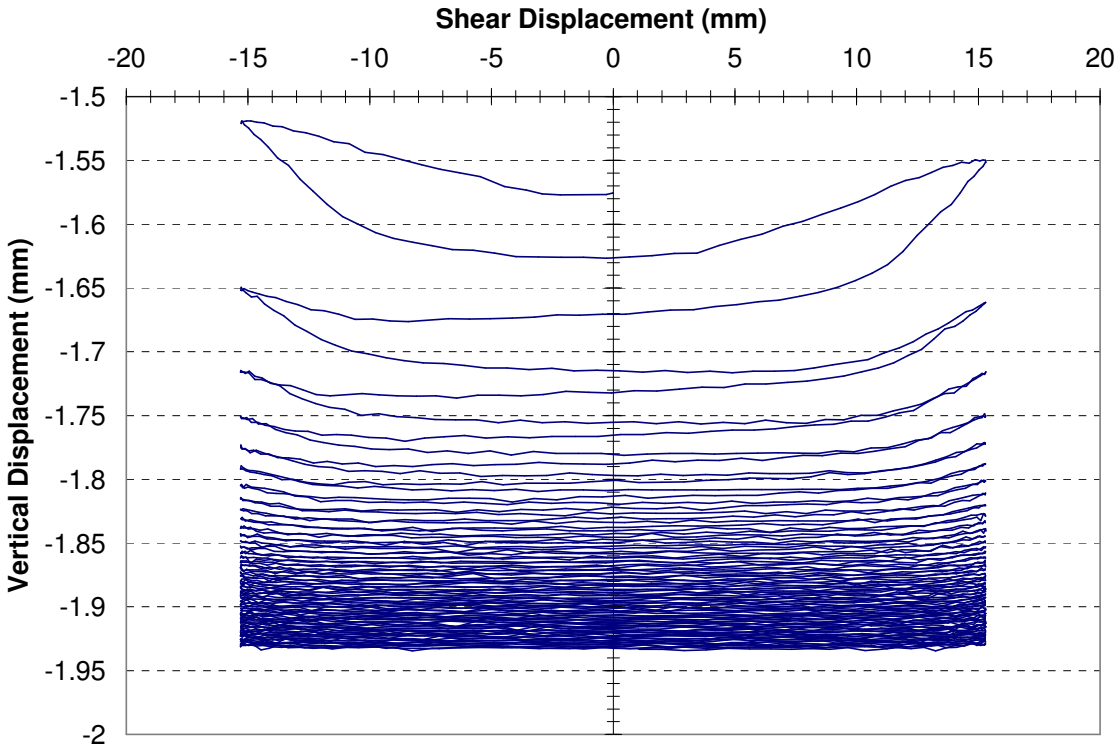

Figure 4.5: Volume change behavior during baseline cyclic shear test.

After allowing the specimen to equilibrate for 24 hours, a static shear test was performed on the specimen. A plot of shear stress versus displacement for this test is

presented in Figure 4.6. Following cyclic shearing at an amplitude of 15 mm, the GCL behaved similarly to a specimen with no previous shearing, with the exception of a reduction in peak shear strength. The effects of displacement amplitude on post-cyclic shear behavior are further discussed in subsequent sections.

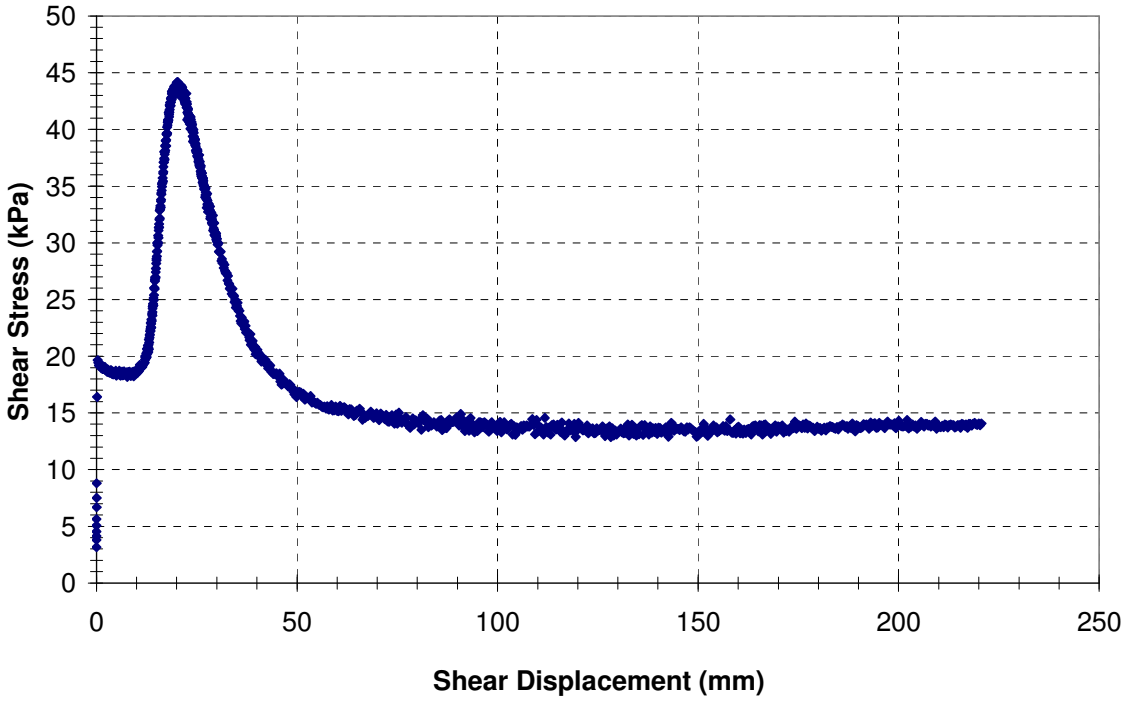

Figure 4.6: Baseline post-cyclic static stress-displacement curve.

4.2.2 EFFECTS OF CYCLIC SHEAR DISPLACEMENT AMPLITUDE

In addition to data from the baseline test (cyclic shear displacement amplitude = 15 mm), plots of shear stress versus time and shear stress versus displacement are presented for displacement amplitudes of 5, 10, 20 and 25 mm. During the 5 mm test (Figure 4.7, Figure 4.8), shear stress reached a much less dramatic peak when compared to the baseline test. This can be attributed to less reinforcement being tensioned during the test. As some reinforcement was engaged and broken, a peak shear stress of 60 kPa

was reached before decreasing to a nearly steady value of 43 kPa by the final cycle. This compares to a peak of 129 kPa and a nearly steady value of 37 kPa by the last cycle of the baseline (15 mm amplitude) test. The same type of behavior was also observed when cyclic shear displacement amplitude was increased to 10 mm (Figure 4.9, Figure 4.10). During the first cycle, shear stress reached a peak of 96 kPa before decreasing to a nearly steady value of 44 kPa. No substantial difference was seen between last-cycle shear strengths for displacement amplitudes of 5 mm and 10 mm (43 kPa and 44 kPa, respectively). Last-cycle shear strength was substantially lower when displacement amplitude was increased to 15 mm (37 kPa).

Shear behavior changed significantly as displacement amplitude exceeded 15 mm. During the 20 mm test (Figure 4.11, Figure 4.12), essentially all of the reinforcement was failed during the first cycle. During the first quarter-cycle, a maximum shear stress of 142 kPa was reached at a displacement of -18 mm, before the specimen was sheared to a maximum displacement of 20 mm. This behavior suggests that nearly all of the reinforcement was broken before maximum displacement was reached. The same behavior occurred during the second half of the first cycle. Shear stress reached a maximum of 101 kPa at a displacement of 14 mm. Shear strength decreased markedly for the 2nd cycle. Shear strength then decreased gradually to 25 kPa by the final cycle.

During the 25 mm shear displacement amplitude test (Figure 4.13, Figure 4.14), this behavior was exaggerated even further. During the first quarter-cycle, shear stress reached a maximum value of 134 kPa at a displacement of -18 mm. In the second half of the first cycle, shear stress significantly decreased to a maximum of 60 kPa at 13 mm of shear displacement. After the 2nd cycle of shearing, the shear strength decreased slowly

to 23 kPa by the final cycle. These results suggest that after 1 cycle of displacement greater than 18 mm, essentially all internal GCL reinforcement has been failed.

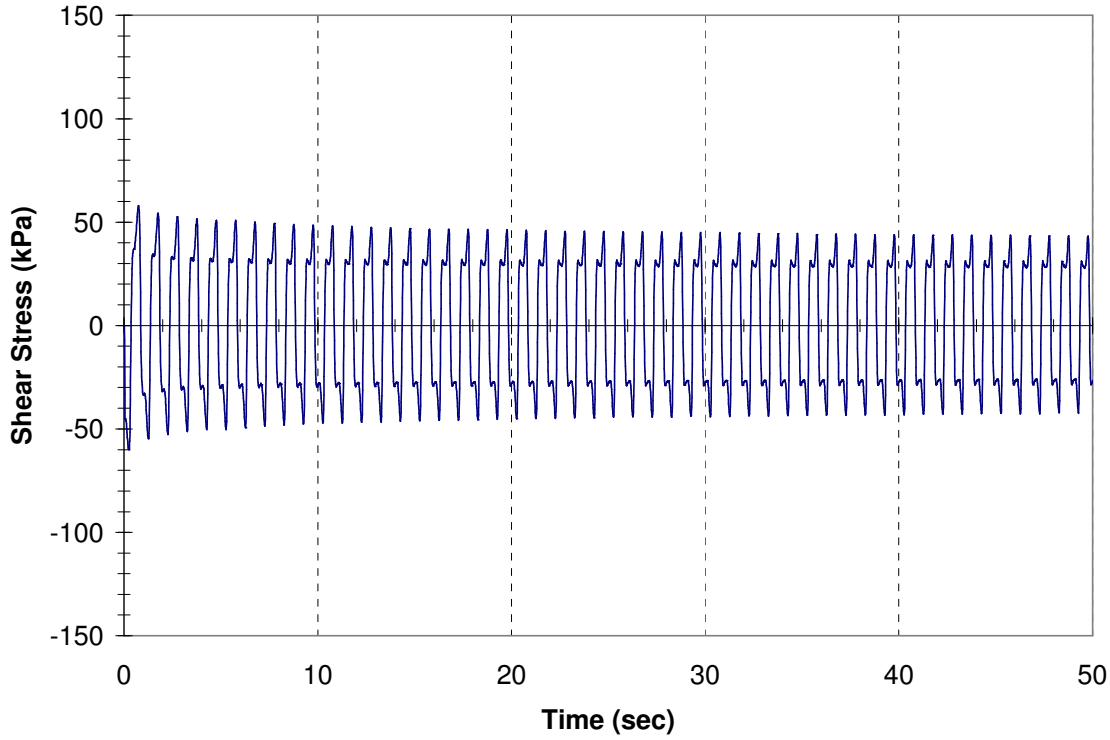

Figure 4.7: Shear stress versus time (Cyclic shear amplitude = 5 mm).

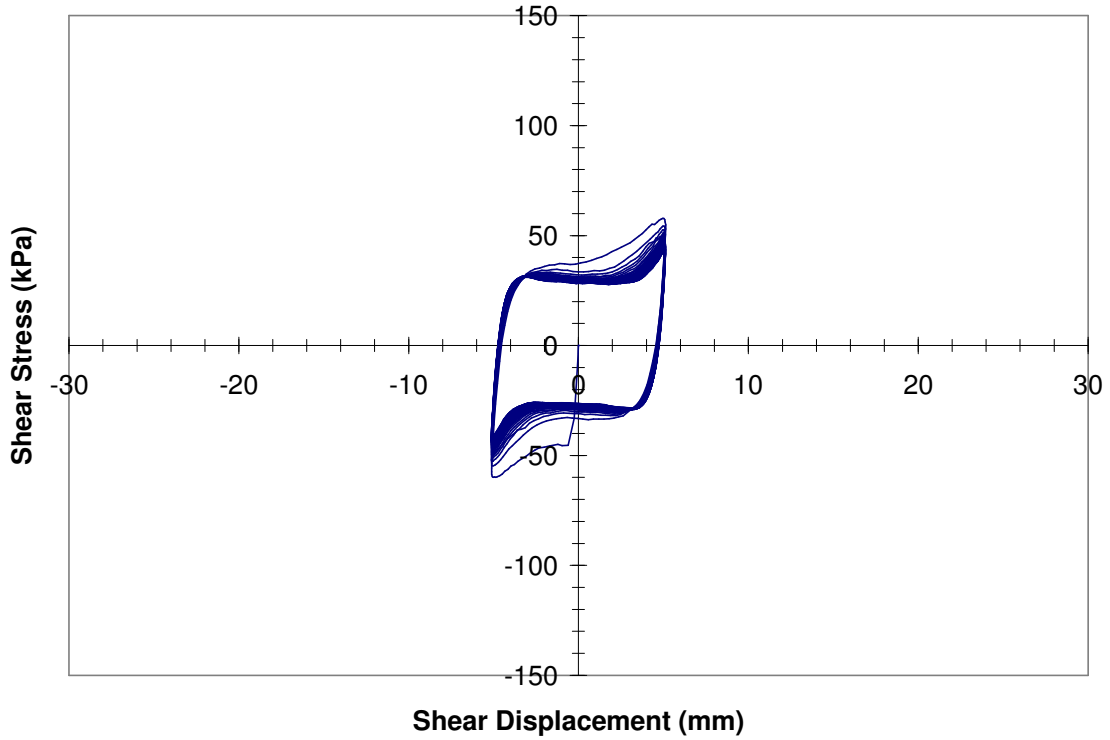

Figure 4.8: Shear stress versus displacement (Cyclic shear amplitude = 5 mm).

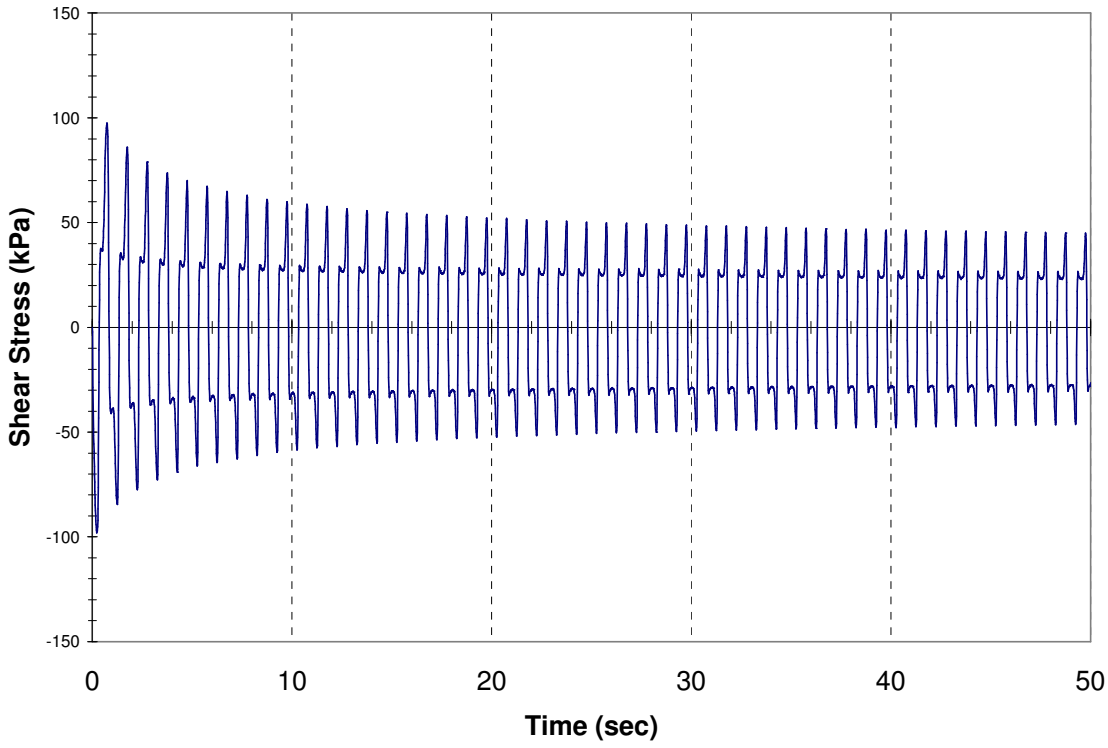

Figure 4.9: Shear stress versus time (Cyclic shear amplitude = 10 mm).

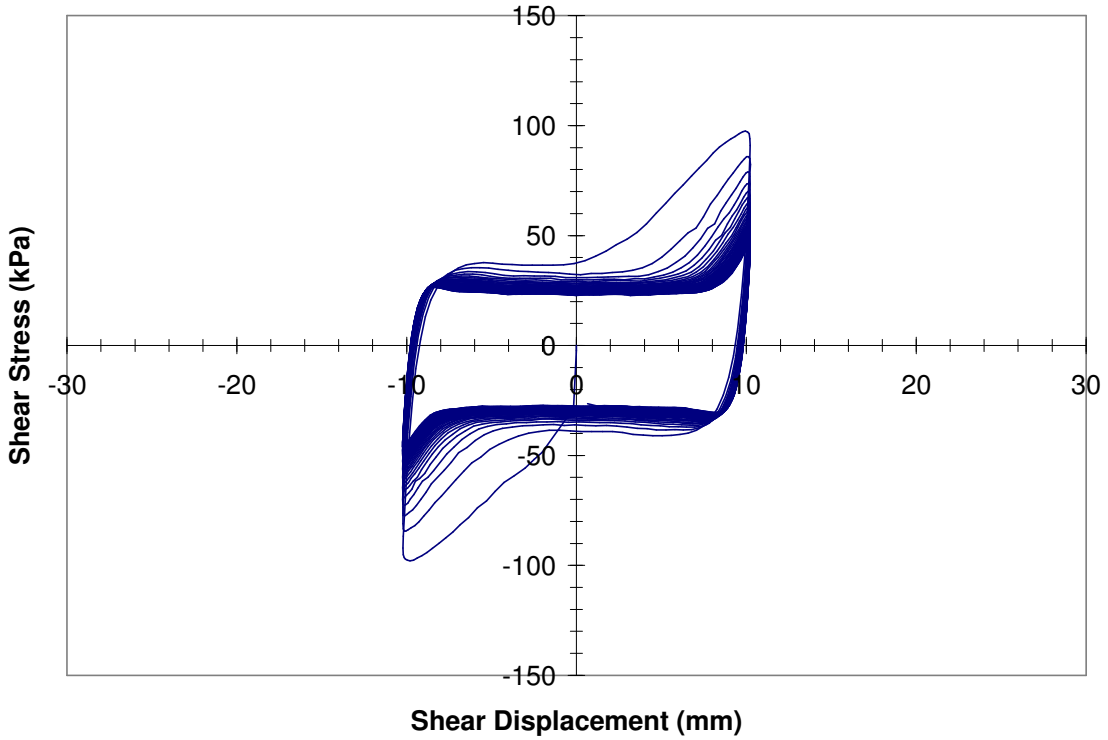

Figure 4.10: Shear stress versus displacement (Cyclic shear amplitude = 10 mm).

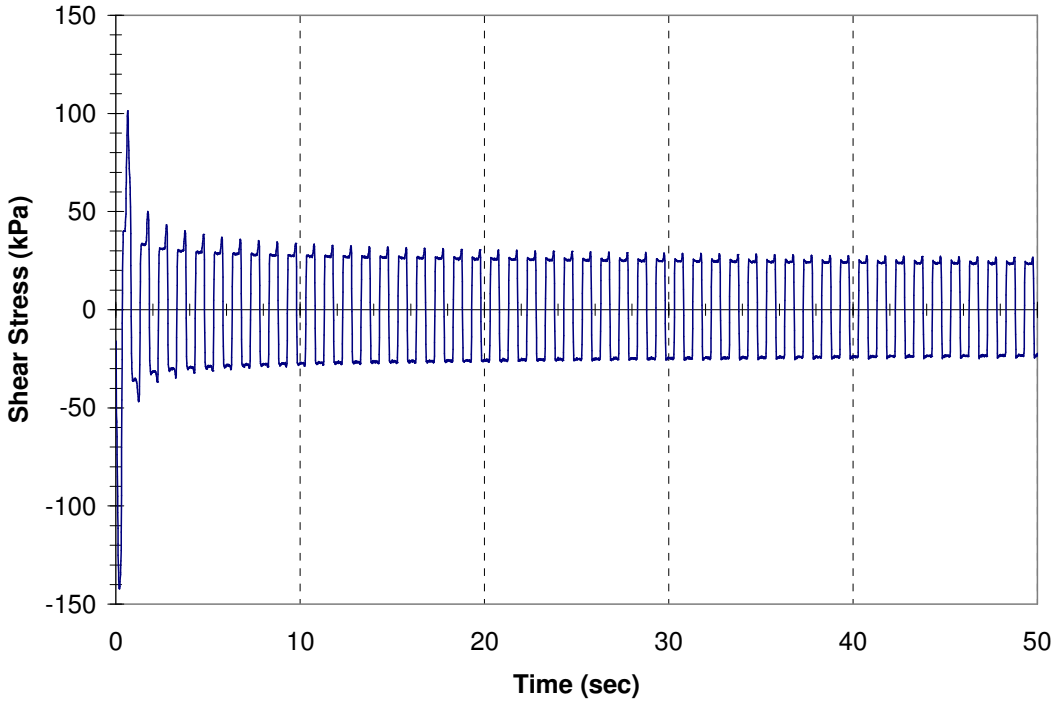

Figure 4.11: Shear stress versus time (Cyclic shear amplitude = 20 mm).

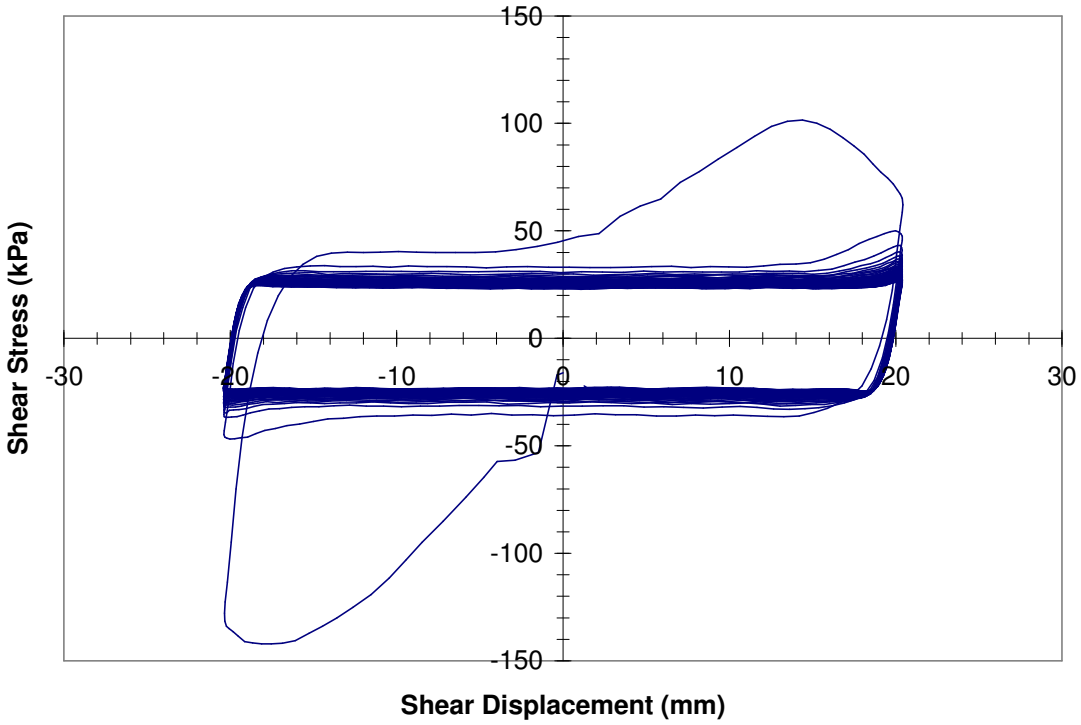

Figure 4.12 Shear stress versus displacement (Cyclic shear amplitude = 20 mm).

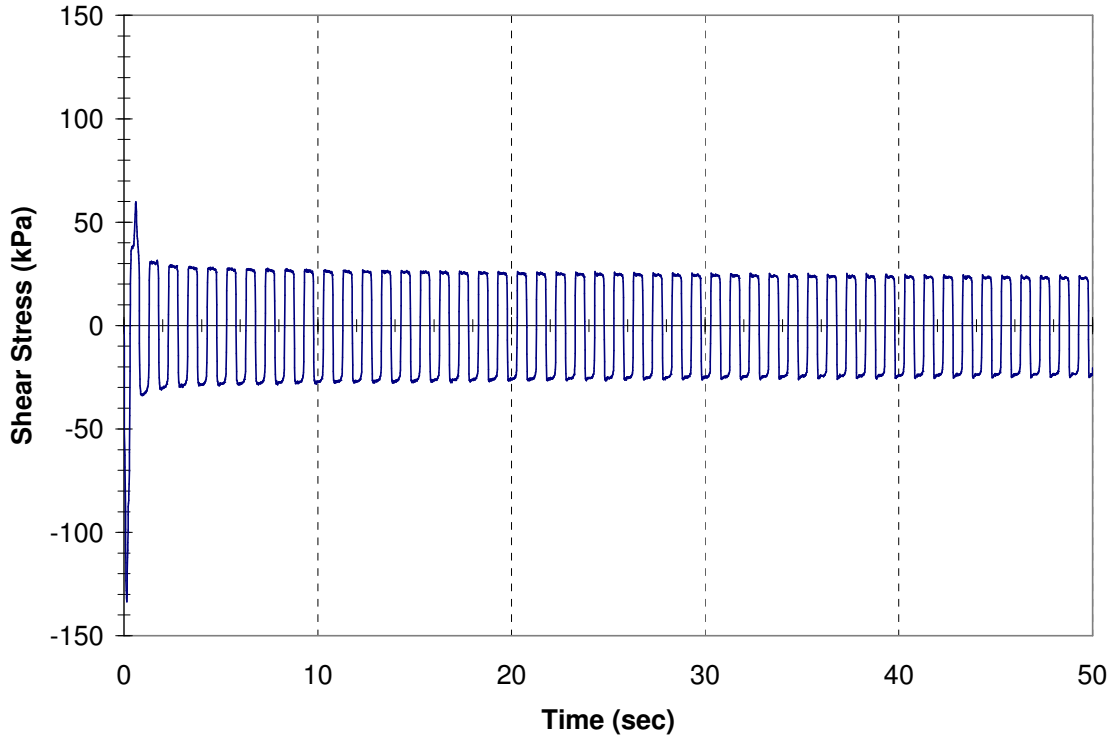

Figure 4.13: Shear stress versus time (Cyclic shear amplitude = 25 mm).

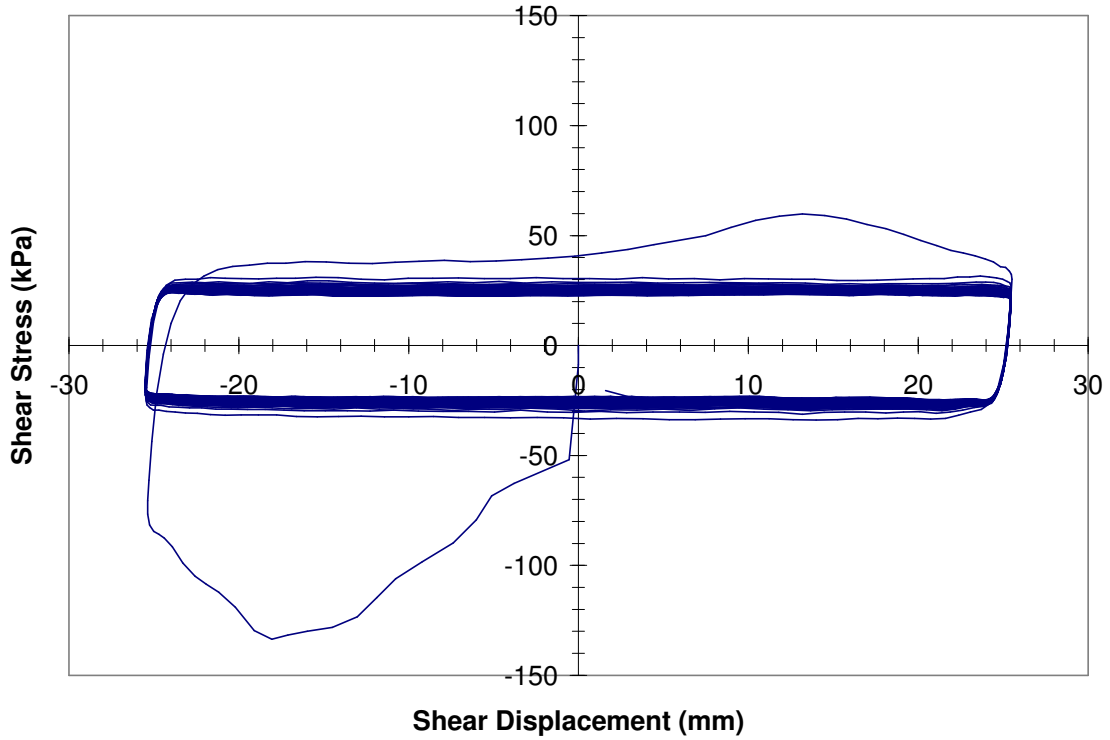

Figure 4.14: Shear stress versus displacement (Cyclic shear amplitude = 25 mm).

In Figure 4.15, the post-dynamic static shear behavior is plotted for each test. It can be seen that as cyclic displacement increased, peak static strength decreased. This weakening is due to less needle-punched reinforcement remaining intact after GCLs are subjected to large cyclic shear displacements. Peak strengths were generally reached at displacements of 18 to 20 mm, which agrees with shear behavior during cyclic shearing. With the exception of the 20 mm and 25 mm tests, the GCLs exhibited distinct strain-softening. In the cases of 20 mm and 25 mm tests, residual or near residual strengths were reached within 30 mm of shearing. Residual strength for all cases seems to be independent of cyclic displacement. This agrees with tests performed by Fox et al. (1997) that showed reinforcing had no effect on residual strength. Residual strength ranged from 12 to 15 kPa for all of the tests. The corresponding residual friction angles ranged from 4° to 5°, which agrees with friction angles of 3° to 5° for bentonite clay reported by Mesri and Olson (1970). After reinforcement has failed, shear behavior of the GCL is governed by the properties of hydrated bentonite clay.

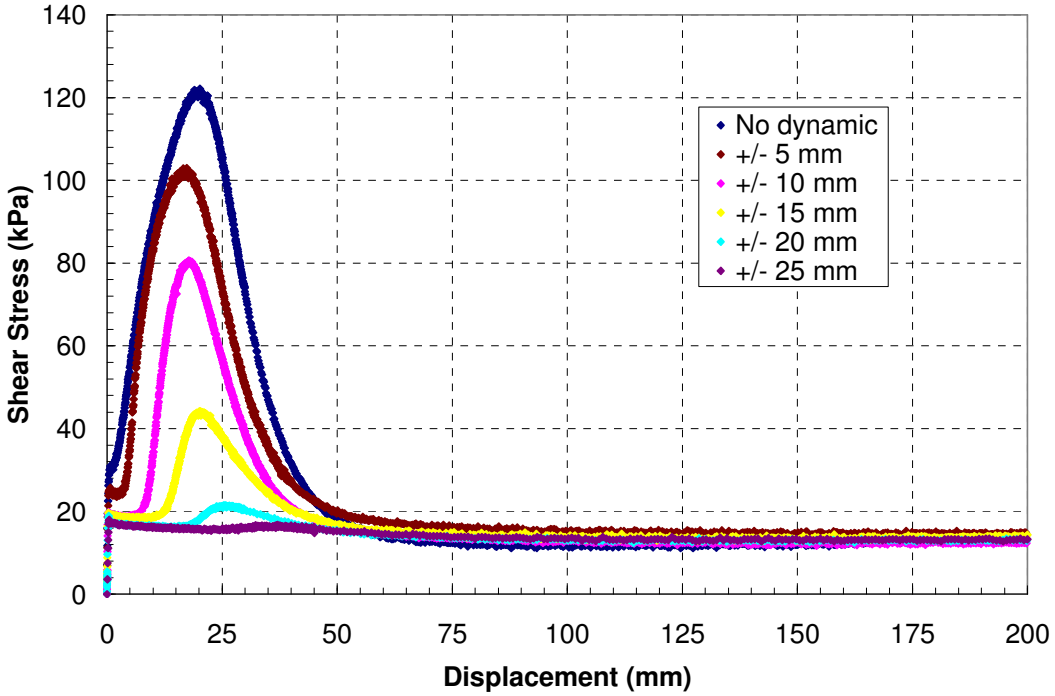

Figure 4.15: Post-dynamic static shear test results.

4.2.3 EFFECTS OF CYCLIC SHEARING FREQUENCY

Cyclic shear tests were conducted at frequencies of 0.1, 0.5, 1.0 and 3.0 Hz, all at a displacement amplitude of 15 mm and for a duration of 50 cycles. With the results from those tests, peak stress per cycle was plotted for each frequency in Figure 4.16. The results suggest that shearing frequency has negligible effects on GCL strength during dynamic loading. The specimen sheared at 1 Hz exhibited slightly higher shear strength than the specimen sheared 3 Hz, however no trend can be established. It is likely that material variability is the cause of variation. However, at such large displacement rates seen during these cyclic tests, very little information is available regarding effects on strength. Further research into this topic is needed.

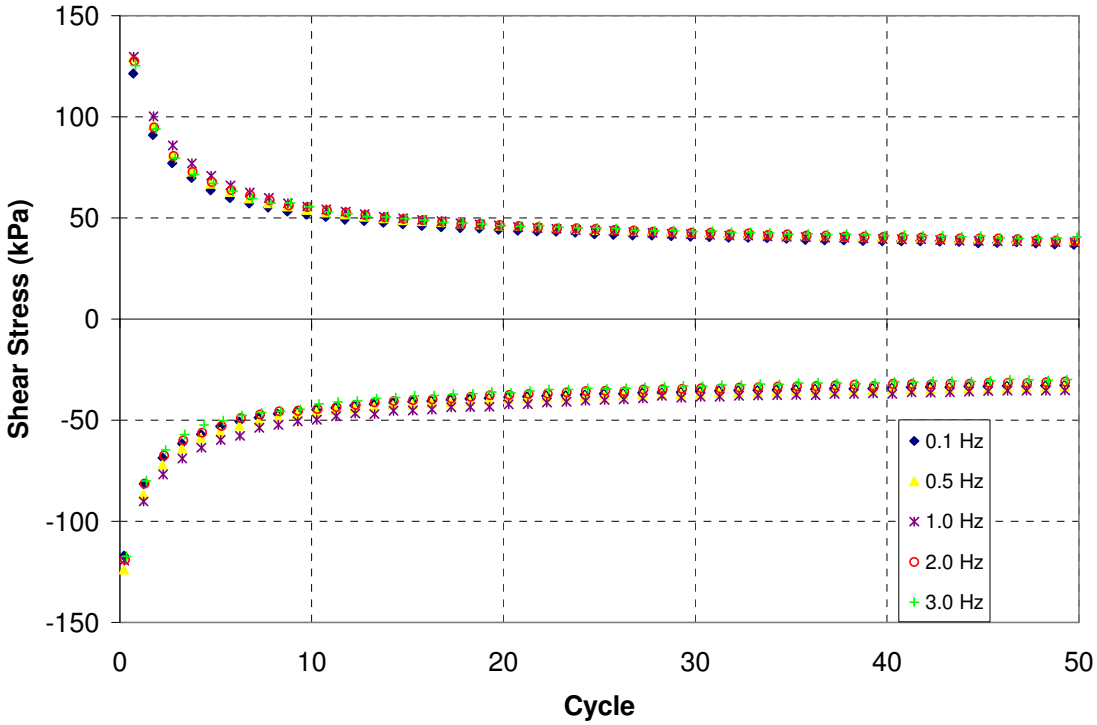

Figure 4.16: Peak shear stress per cycle.

Post-dynamic peak and residual shear strengths are plotted as a function of excitation frequency in Figure 4.17. Between 0.5 Hz and 2 Hz, peak static shear strength increased to a maximum of 47 kPa at a frequency of 2 Hz. Peak strength decreased to 35 kPa at 3 Hz. A similar trend was also seen in the residual strength values.. These results suggest that as cyclic shear displacement rate is increased, shear strength increases until a point between 2 Hz and 3 Hz, and then begins to decrease with increasing shear frequency. While Eid et al. (1999) observed shear strength to increase with increasing displacement rate up to 30 mm/min., a cyclic shear frequency of 0.1 Hz with a displacement amplitude of 15 mm corresponds to an average displacement rate of 360 mm/min. Discrepancies in the correlation between shear frequency and post-cyclic static

strength are most likely due to material variability. Further research is needed to examine this trend.

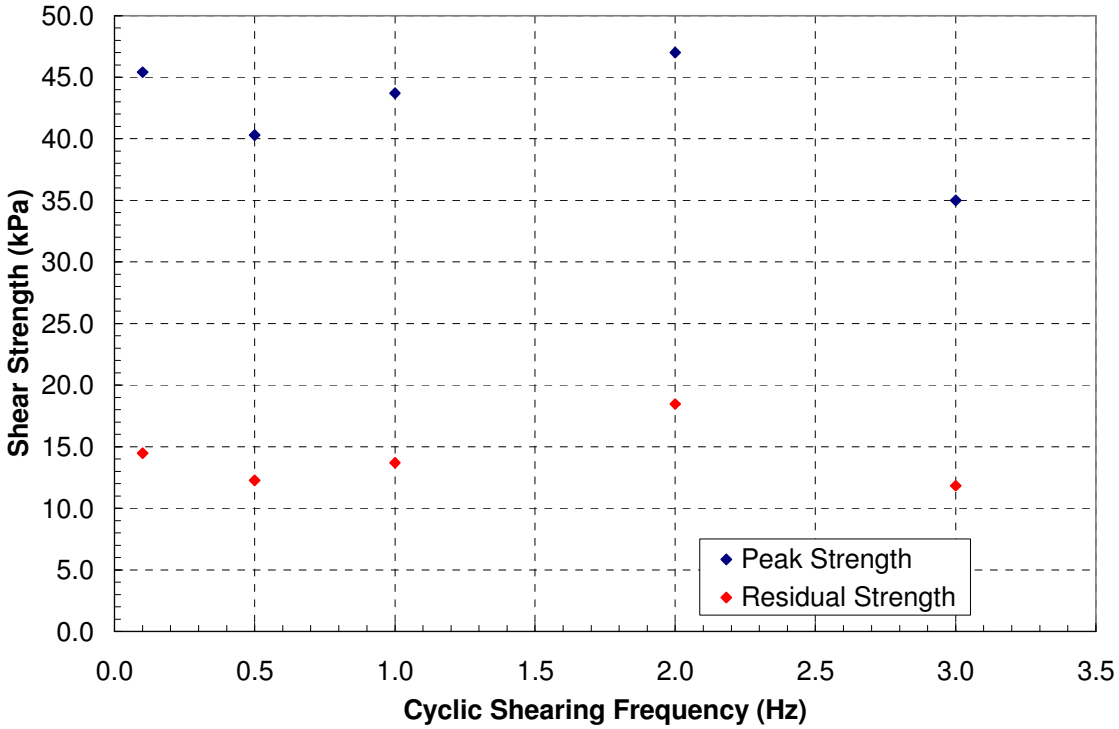

Figure 4.17: Post-cyclic static shear strength as function of frequency.

4.2.4 EFFECTS OF TOTAL NUMBER OF SHEAR CYCLES

After performing the baseline test at a shear displacement amplitude of 15 mm for 50 cycles at 1 Hz, other tests were performed at the same displacement amplitude and frequency for 10 and 100 cycles. The post-cyclic static peak and residual strengths from these tests are plotted in Figure 4.18. After shearing the GCL for 10 cycles, gains were seen in static peak strength when compared to the 50 cycle and 100 cycle tests. This agrees with results presented in section 4.2.2. As the specimen is sheared for more cycles, more reinforcement is degraded and a gradual decrease in strength is seen. Post-cyclic residual strengths remained independent of the number shear cycles. This is to be

expected, as all reinforcement has failed during at residual conditions and GCL strength is nearly that of hydrated bentonite (Chiu and Fox 2004, Zornberg et al. 2005).

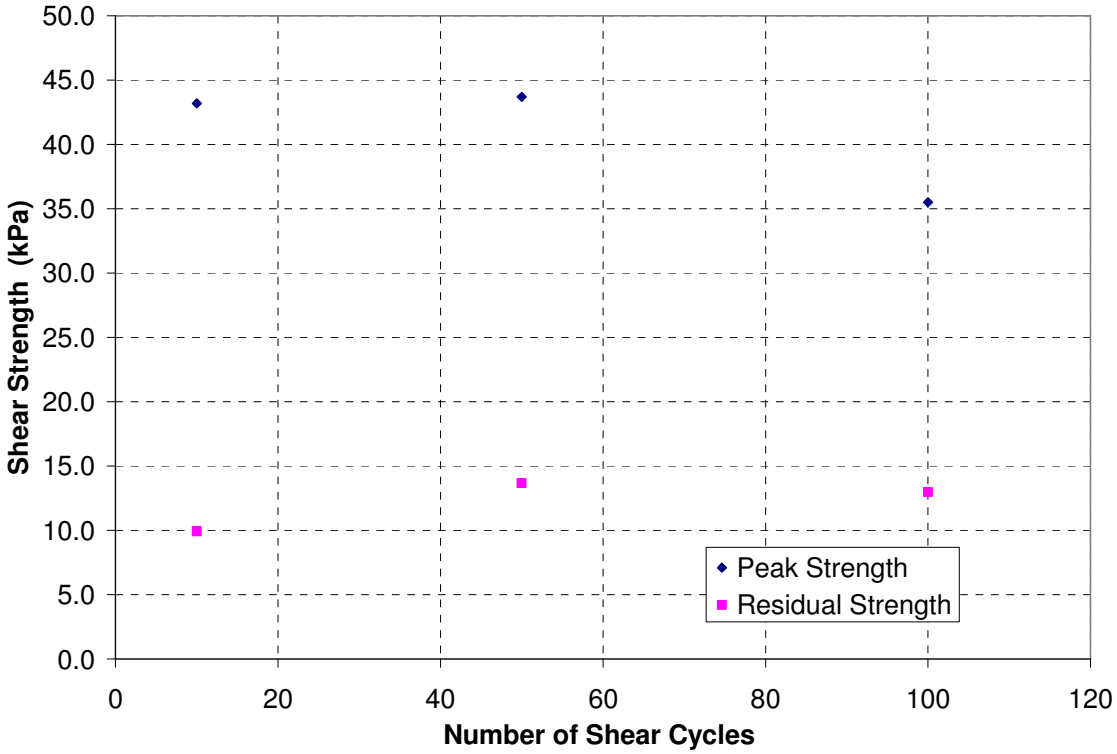

Figure 4.18: Post-cyclic static strength as a function of number of cycles.

CHAPTER 5

CONCLUSIONS

The primary objective of this research was to begin investigating the dynamic shear behavior of a reinforced NP GCL. For this study, Bentomat ST manufactured by CETCO (Arlington Heights, Illinois) was selected for research. Displacement-controlled cyclic shear tests were performed using a state-of-the-art dynamic direct shear machine. As part of the testing program, parameters such as cyclic shear displacement amplitude, shearing frequency and number of shearing cycles were varied to study the dynamic and post-dynamic shear behavior of an NP GCL.

The results of this research suggest cyclic shear displacement amplitude has significant effects on both the dynamic and post-cyclic shear strength of NP GCLs. Post-cyclic static strength decreases as cyclic displacement amplitude increases. This behavior is largely dependent on the performance of needle-punched reinforcement. The effects of cyclic shearing frequency are less important. Results suggest post-cyclic static shear strength increases with cyclic shearing frequency up to a certain point at which significant decreases in shear strength occur. To better understand this effect, research should be conducted studying the behavior of GCLs sheared under high displacement rates. The results of this research have also shown that post-cyclic shear behavior is very

dependent on the number of shearing cycles. Shear strength decreases non-linearly with continuing cycles until all needle-punched reinforcement has been failed.

Future research into the dynamic behavior of GCLs can help provide relationships for shear modulus reduction and damping ratio that are needed for ground response analysis. As the capabilities of the dynamic direct shear machine become better understood, various types of tests, including stress controlled tests, can be completed to better understand the dynamic shear behavior of GCLs and GCL interfaces. The results from those tests can be applied to improve understanding of the long-term performance of landfill liner systems constructed in seismic regions

LIST OF REFERENCES

ASTM D 5321 (2002). Test Method for Determining the Coefficient of Soil and Geosynthetic or Geosynthetic and Geosynthetic Friction by the Direct Shear Method, American Society for Testing and Materials, Philadelphia, Pennsylvania.

ASTM D 6243 (1998). Test Method for Internal and Interface Shear Resistance of Geosynthetic Clay Liner by the Direct Shear Method, American Society for Testing and Materials, Philadelphia, Pennsylvania.

Chiu, P. and Fox, P.J. (2004). "Internal and Interface Shear Strengths of Unreinforced and Needle-Punched Geosynthetic Clay Liners," *Geosynthetics International*, Vol. 11, No. 3, pp. 176-199.

De, A. and Zimmie, T.F. (1998). "Estimation of Dynamic Interfacial Properties of Geosynthetics," *Geosynthetics International*, Vol. 5, No. 1-2, pp. 17-39.

Eid, H.T. and Stark, T.D. (1997). "Shear Behavior of an Unreinforced Geosynthetic Clay Liner," *Geosynthetics International*, Vol. 4, No. 6, pp. 645-659.

Eid, H.T., Stark, T.D. and Doefler, C.K. (1999). "Effect of Shear Displacement Rate on Internal Shear Strength of a Reinforced Geosynthetic Clay Liner," *Geosynthetics International*, Vol. 6, No. 3, pp. 219-239.

Fox, P.J., Nye, C.J., Morrison, T.C., Hunter, J.G. and Olsta, J.T. (2006). "Design and Evaluation of a Large Dynamic Direct Shear Machine for Geosynthetic Clay Liners," *Geotechnical Testing Journal*, in press.

Fox, P.J., Rowland, M.G. and Scheithe, J.R. (1998). "Internal Shear Strength of Three Geosynthetic Clay Liners," *Journal of Geotechnical and Geoenvironmental Engineering*, Vol. 124, No. 10, pp. 933-944.

Fox, P.J., Rowland, M.G., Scheithe, J.R., Davis, K.L., Supple, M.R. & Crow, C.C. (1997). "Design and Evaluation of a Large Direct Shear Machine for Geosynthetic Clay Liners," *Geotechnical Testing Journal*, Vol. 20, No. 3, pp. 279-288.

Fox, P.J. and Stark, T.D. (2004). "State-of-the-art report: GCL Shear Strength and its Measurement," *Geosynthetics International*, Vol. 11, No. 3, pp. 141-175.

Gilbert, R.B., Liu, C.N., Wright, S.G. and Trautwein, S.J. (1995). "A Double Shear Test Method for Measuring Interface Strength," *Proceedings*, Geosynthetics 95, pp. 1017-1029.

Gilbert, R.B., Fernandez, F. and Horsfield, D.W. (1996). "Shear Strength of Reinforced Goesynthetic Clay Liner," *Journal of Geotechnical and Geoenvironmental Engineering*, Vol. 122, No. 4, pp. 259-266.

Gilbert, R.B., Scranton, H.B. and Daniel, D.E. (1997). "Shear Strength Testing for Geosynthetic Clay Liners," *Testing and Acceptance Criteria for Geosynthetic Clay Liners, STP 1308*, ASTM International, West Conshohocken, Pennsylvania, pp. 121-135.

Kim, J., Riemer, M. and Bray, J.D. (2005). "Dynamic Properties of Geosynthetic Interfaces," *Geotechnical Testing Journal*, Vol. 28, No. 3, pp. 1-9.

Lai, J., Daniel, D.E. & Wright, S.G. (1998). "Effects of Cyclic Loading on Internal Shear Strength of Unreinforced Geosynthetic Clay Liner," *Journal of Geotechnical and Geoenvironmental Engineering*, Vol. 124, No. 1, pp. 45-52.

Lo Grasso, S.A., Massimino, M.R. and Maugeri, D.I.C.A (2002). "Dynamic Analysis of Geosynthetic Interfaces by Shaking Table Tests," *Proceedings, 7th International Conference on Geosynthetics*, Nice, Vol. 4, pp. 1335-1338.

Mesri, G. and Olson, R.E. (1970). "Shear Strength of Montmorillonite," *Geotechnique*, Vol. 20, No. 3, pp. 261-270.

Nye, C. J. (2006). "Research on dynamic internal shear strength of a needle-punched geosynthetic clay liner," MS thesis, College of Engineering, The Ohio State University, Columbus, Ohio.

Rowland, M. G. (1997). "Research on the internal shear strength of three geosynthetic clay liners," MS thesis, School of Civil Engineering, Purdue University, West Layfayette, Indiana.

Scheithe, J. R. (1996). "Research on the internal shear strength of a needle-punched geosynthetic clay liner," MS thesis, School of Civil Engineering, Purdue University, West Lafayette, Indiana.

Stark, T.D. and Poeppel, A.R. (1994). "Landfill Liner Interface Strengths from Torsional-Ring-Shear Tests," *Journal of Geotechnical Engineering*, Vol. 120, No. 3, pp. 597-615.

Stark, T.D. and Eid, H.T. (1996). "Shear Behavior of Reinforced Geosynthetic Clay Liners," *Geosynthetics International*, Vol. 3, No. 6, pp. 771-786.

Triplett, E.J. and Fox, P.J. (2001). "Shear Strength of HDPE Geomembrane/Geosynthetic Clay Liner Interfaces," *Journal of Geotechnical and Geoenvironmental Engineering*, Vol. 127, No. 6, pp. 543-552.

USEPA (1995). "RCRA Subtitle D (258) seismic design guidance for municipal solid waste landfill facilities," by G. N. Richardson, E. Kavazanjian, Jr., and N. Matasovi, EPA/600/R-95/051, April.

Yegian, M.K. and Lahlaf, A.M. (1992). "Dynamic Interface Shear Strength Properties of Geomembranes and Geotextiles," *Journal of Geotechnical and Geoenvironmental Engineering*, Vol. 118, No. 5, pp. 760-779.

Yegian, M.K. and Kadakal, U. (1998). "Geosynthetic Interface Behavior Under Dynamic Loading," *Geosynthetics International*, Vol. 5, No. 1, pp. 1-16.

Yegian, M.K., Yee, Z.Y. and Harb, J.N. (1995). "Seismic Response of Geosynthetic/Soil Systems," *Geoenvironmental 2000*, Geotechnical Special Publication No. 46, ASCE, Vol. 2, pp. 1113-1125.

Zornberg, J.G., McCartney, J.S. and Swan, R.H. (2005). "Analysis of a Large Database of GCL Internal Shear Strength Results," *Journal of Geotechnical and Geoenvironmental Engineering*, Vol. 131, No. 3, pp. 367-380.